



OPEN Therapeutic efficacy of BSA formulated hydrogels in corneal wound healing and epithelial cell regeneration: an ex vivo study

Ramachandran Samivel^{1✉}, Mana A. Alanazi¹, Adnan A. Khan¹, Ali M. Masmali¹, Saud A. Alanazi¹, Turki Almubrad¹ & Saeed Akhtar^{2✉}

Corneal injury requires both epithelial regeneration and stromal repair, and formulated biomaterials established to repair damaged corneas can be used in regenerative medicine. The challenge is to ensure that biomaterials can be incorporated into the host tissue and delivered intracellularly without causing rapid material deprivation, thus maintaining corneal transparency. Bovine serum albumin-formulated hydrogels (BHG) were prepared by dissolving with riboflavin, retinoic acid, and 2.5% glutaraldehyde solutions. Periphery-centered wounds from camel corneas (8mm diameter and 250 µm depth) were mounted on a dome-shaped agarose gel in six-well plates containing BHG-supplemented serum-free Medium 199. The plates were then incubated at 37 °C for 24, 48, and 72 h. A complete set of corneoscleral rings was procured and processed for histopathological, electron microscopy, and immunohistochemistry assays. Histological and electron microscopy results showed that all epithelial layers and anterior stroma developed faster in the BHG-treated wounds than in the untreated wounded corneas. Compared to untreated wounded corneas, BHG-treated corneas accumulated higher levels of fibronectin and ki-67 and lower levels of alpha-smooth muscle actin inductions. BHG-treated corneal wounds healed faster than untreated wounded corneas. Overall, BHG enhances epithelial regeneration and strengthens the stromal architecture by upregulating ECM and growth factors. Hence, BHG is a promising therapeutic hydrogel for wounded corneas, and further studies on corneal stromal wound healing and epithelial cell reimbursement in an in vivo model are required.

Keywords Hydrogel, Retinoic acid, Riboflavin, Bovine serum albumin, Corneal-sclera, Organ culture

Abbreviations

BSA	Bovine serum albumin
RF	Riboflavin
RA	Retinoic acid
GA	Glutaraldehyde
BHG	Bovine serum albumin-riboflavin-retinoic acid-formulated hydrogel
PS	Penicillin-streptomycin
EP	Epithelium
S	Stroma
TF	Tear film
BM	Basement membrane
CFs	Collagen fibrils
PSC	Progenitor stem cell
DAPI	4',6-Diamidine-2'-phenylindole dihydrochloride
α-SMA	Alpha smooth muscle actin
PDGFRα	Platelet-derived growth factor receptor-α
TGF	Transforming growth factor
PBST	Phosphate buffered saline-Tween 20

¹Cornea Research Chair, Department of Optometry, College of Applied Medical Sciences, King Saud University, Riyadh, Saudi Arabia. ²College of Applied Medical Sciences, Inaya Medical Sciences, Riyadh, Saudi Arabia. ✉email: rkumari@ksu.edu.sa; sakhtar@inaya.edu.sa

The cornea is a transparent, multilayered tissue with avascular vessels that serve as a barrier against external influences such as air, sunlight, chemical substances, desiccants, and microbes¹. It consists of five layers: epithelium, Bowman's membrane, stroma, Descemet's membrane, and endothelium². The stroma contains uniformly distributed collagen fibrils (CFs) and proteoglycans (PGs), which provide strength and transparency³. In humans, the cornea measures 11.5 mm in diameter, 0.45–0.6 mm thick in the center, and 0.6–0.8 mm thick at the periphery. However, camels have a 29.8 mm corneal diameter and a thickness ranging from 0.9 to 1.2 mm in the center to 1–1.3 mm at the periphery⁴. The human epithelium comprises approximately 9% of the cornea, whereas the camel epithelium comprises approximately 36% of the cornea⁴. The surface of the camel epithelium is covered by the glycocalyx (1.5 μm) and contains 13 layers, including squamous cells, wing cells, and basal cells⁴. Basal epithelial cells are very large, columnar, and are attached to the basal lamina or basal membrane, followed by collagen fibrils. The basement membrane is an acellular extracellular matrix composed of two layers: lamina lucida and lamina densa⁵. The basement membrane is composed of collagen, laminin, heparan sulfate (HSPG), and nidogens. It also contains many other components, such as fibronectin, thrombospondin-1, and matrilin-4⁶.

Riboflavin (RF) and retinoic acid (RA) are non-toxic bioactive molecules that act as photoinitiators upon exposure to visible ultraviolet light (320–450 nm). Riboflavin has been widely used as a photosensitizing agent for corneal cross-linking, which leads to the formation of covalent bonds between collagen fibrils in the corneal stroma⁷. RF upregulates transglutaminase-2 (TG2), a key enzyme involved in wound healing response, adhesion, proliferation, and migration of epithelial cells in both humans and mice^{8–10}. Similarly, RA is crucial for maintaining corneal stem cell proliferation and differentiation to create a healthy cornea and prevent corneal aging¹¹. Experiments on RA are crucial for studying cellular differentiation, homeostasis, organ development, and eye health^{12–14}. RA also plays an important role in eye development through the regulation of Wnt– β -catenin signaling, which is involved in the formation of corneal stromal cells¹⁵.

Earlier, Kumar et al. reported that RA is a biologically active metabolite that is essential for the development of eye morphogenesis and maintenance of the endogenous enzyme recruiting gene *Aldh1a1*. Conditional knockout of *Aldh1a1* and RA deficiency mice reduced corneal thickness, and the epithelium and stroma were very thin¹⁶. Furthermore, other studies have suggested that RA is a potent source of vitamin A (retinol) and may play an important role in vision by balancing antioxidants and epigenetic regulators, promoting embryonic assembly, increasing cell proliferation, and reprogramming stem cell differentiation¹⁷. Another, well-known biologically active endogenous molecule for keratoconus corneal cross-linking is RF, because it enhances permeability and radiosensitizes biologically active molecules to translocate into deeper tissues¹⁸. RF is an essential endogenous enzyme for growth and development because it converts FMN and FAD, which are essential cofactors in carbohydrate, protein, and lipid metabolism¹⁹. Bhattacharjee et al.²⁰ discovered that the covalently coupled bioactive molecules RF and RA combined with silk fibroin (SF) bioengineered scaffolds (matrices) positively influence corneal stromal keratocyte cell behavior, including cell adhesion, proliferation, ECM formation, and keratocyte-associated gene expression.

The current study established that bovine serum albumin (BSA) can form nanocarriers, which can be used to transport drugs efficiently²¹. This is due to the fact that BSA is a natural protein capable of forming complexes of different shapes. Proteins, such as BSA, are highly biocompatible, biodegradable, nontoxic, and nonimmunogenic²². Albumin, which is the most abundant plasma protein in mammals, is a versatile and easily obtainable biomaterial. Because it responds to pH and temperature, it readily dissolves in high concentrations and gels under defined conditions. Albumin is an attractive biomaterial for biomedical research and therapeutics because of its versatility, low cost, and biocompatibility. In clinical research, albumin has mainly been used as a carrier molecule or nanomaterial to improve drug pharmacokinetics and delivery^{23,24}.

This study aimed to synthesize and optimize the bioactive molecules riboflavin (RF) and retinoic acid (RA) with BSA hydrogel formulations at different concentrations. The study hypothesized that biomolecules combined with BSA-hydrogel would result in enhanced corneal epithelial cell regeneration in an ex vivo wound healing model. Therefore, this study was carried out to investigate the effectiveness of a formulated BSA hydrogel containing riboflavin (RF) and retinoic acid (RA) in healing the corneal epithelium and its remodeling. The combined delivery of both biomolecules has not been explored previously, especially when using BSA-formulated hydrogels. To the best of our knowledge, this is the first study to show the ultrastructural development of the epithelium, basal cells, and anterior stromal collagen fibrils in a wounded cornea.

Methods

Preparation of riboflavin (RF)-retinoic acid (RA) formulated BSA hydrogel (BHG)

Bovine serum albumin (A4161, Sigma-Aldrich) at three different concentrations (5, 10, and 20%) was dissolved in 5 mL of distilled water at pH 7.4. Then, 20 mg/dL riboflavin (R7774, Sigma-Aldrich), 25,000 IU/dL retinoic acid (R2625, Sigma-Aldrich), and 20 μL of 2.5% glutaraldehyde (G7651, Sigma-Aldrich) were added to the BSA solution and stirred well for 12 h at room temperature. The undissolved particles from the solutions were removed by membrane dialysis using a molecular weight cut-off of 20 kDa (MD77, Membra-Cel). The dialyzed BSA hydrogel suspensions were subsequently stored at 4 °C until further analysis (Fig. 1A). As shown in Fig. 1B, the synthesized BSA hydrogels were resuspended and their absorption spectra were scanned (200–800 nm) using UV–visible spectrophotometry. The biomechanical properties and crosslinking natures of the 10% and 20% BSA hydrogels were similar. Although the optical density of the absorption spectrum is higher, we chose to conduct further experiments on 10% BHG on the basis of the results of the BHG solution viscosity and UV–visible absorption spectral analysis, since 10% BSA was more suitable for in vitro cell culture and tissue penetration.

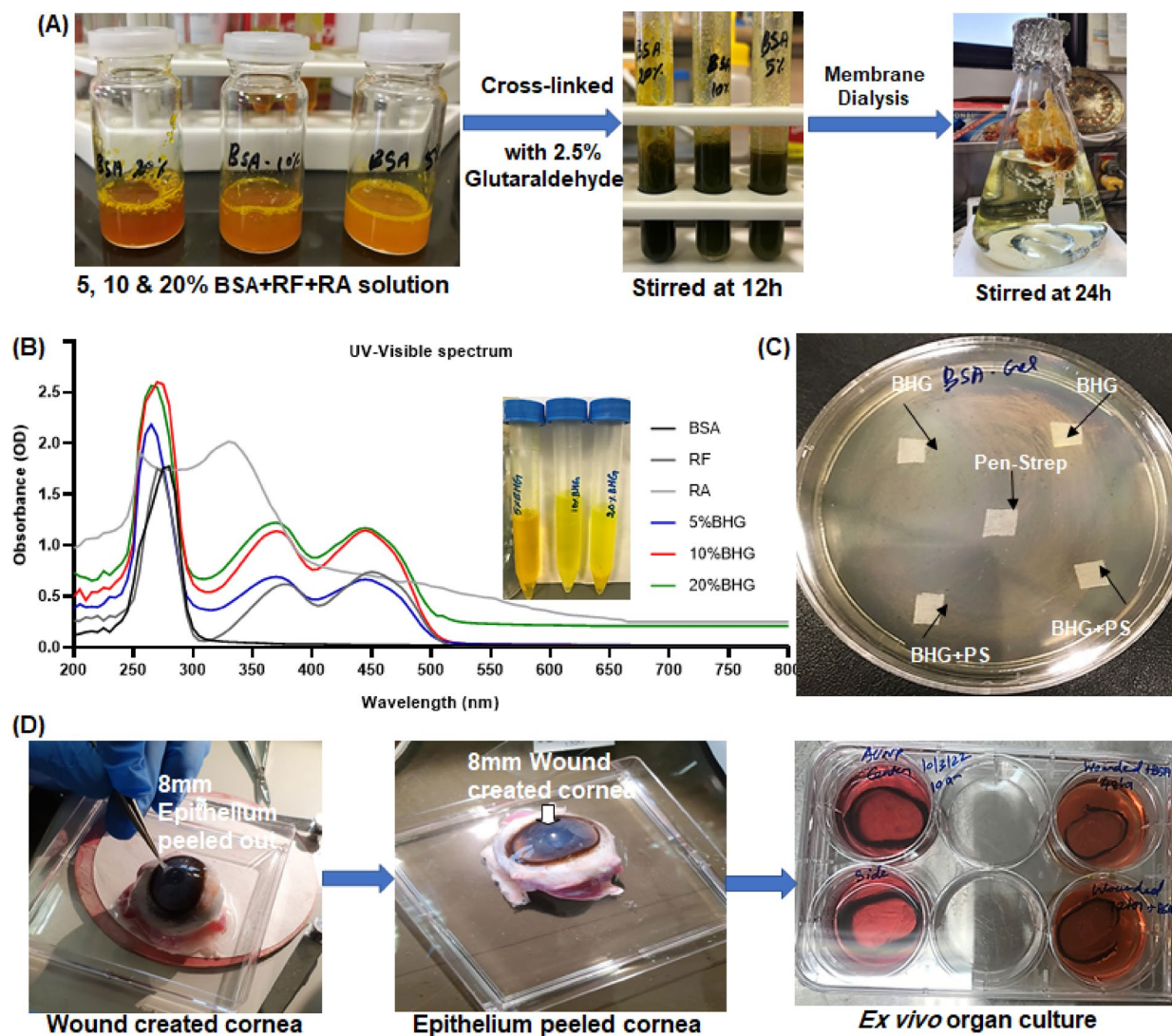


Fig. 1. (A) Step 1: RA and RF were mixed with three different concentrations (5%, 10%, and 20%) of BSA solutions. Step 2: in the solution, glutaraldehyde was added to hydrogel formation with continuous stirring, and step-3 followed by membrane dialysis to remove unreacted excess solute particles; (B) The graph shows UV-Vis absorption spectral analysis of 5%, 10%, and 20% BHG, and the centrifuge tubes shows the resuspended BHG solution viscosity; (C) Plates shows sterility of BHG, BHG + PS, and PS solution soaked discs on agar plate; (D) Steps 1 and 2 shows to create the wound, an 8 mm diameter trephine was carefully punched into the cornea's center, and the 8 mm wounded epithelium was peeled out. Step-3 An ex vivo organ culture setups were used to incubate the wounded and the wounded with BHG treatment at 24, 48, and 72 h.

Assessment of sterility of the BSA-hydrogel (BHG)

Whatman filter paper discs were treated with 10% BHG and 10% BHG + 0.1% penicillin–streptomycin (PS). All tissue disks were placed on a 10 × 75 mm MacConkey agar plate and incubated for one week at 37 °C. Bacteria or other organisms did not contaminate the discs. Figure 1C shows the sterility test by placing a disc soaked in BHG, BHG + PS, or PS on an agar plate. The agar plate test confirmed the sterility of BHG.

Sample collection and corneal wound creation

Camel eyes were obtained from a local abattoir within 4 h of slaughter and transported to the laboratory on ice. In this study, eight healthy male camel eyes from four camels weighing 60–75 kg and 2–4 years old in the Riyadh region of Saudi Arabia were examined in each set of experiments. A total of 24 corneas were used in this study, consisting of three sets of experiments. For the culture setup, the eyeballs were anatomically examined by an ophthalmologist at King Saud University Hospital for their appearance, dimensions, and location to ensure that the corneas were clinically healthy. Tissue procurement was performed in accordance with the Declaration of Helsinki and local regulations. This study was recommended by the local committee of King Saud University and was conducted accordingly. The eye globes were freed of excess muscle and connective tissue and placed within a disinfectant solution (1% penicillin/streptomycin in PBS with amphotericin B) for 10 min.

The ex vivo organ cultures were grown from corneoscleral explants using a modification of a previously described method Castro et al. 2019²⁵. In brief, the entire corneoscleral ring was rinsed with a PBS solution containing 1% Penicillin–Streptomycin and 1.25 µg/mL Amphotericin B. To create the corneal wound, a trephine of 8 mm diameter was carefully punched into the center of the cornea. In this case, the trephine penetrated the epithelium and anterior stroma without creating a full-thickness corneal wound. The trephine was inserted carefully in the center of the cornea. It rotated 180° clockwise and counterclockwise 2 × as light pressure was applied to deepen the wound (approximately 8 mm diameter and 250 µm deep). Once the wound was deep enough, a pair of fine forceps was used to lift a flap of tissue under the supervision of an inverted surgical microscope. On the other hand, use a knife cutting parallel to the globe to cut away the tissue as the forceps continue to lift off the anterior cornea within the wound margin, as the flap is lifted from the edges. Following this step, a circular wound appeared at the center of the cornea, as shown in Fig. 1D.

Corneal ex vivo organ culture

The control and wound-created corneoscleral rings were placed on the epithelial side down in sterile cups, and the endothelial side of the corneal cavity was filled with warmer 1% agarose containing medium 199 (31150030, Gibco) and 1% antibiotic–antimycotic solution and allowed to freeze. The corneoscleral rings were then inverted and transferred to 6-well culture plates by adding 2 mL of medium 199 supplemented with 10% BHG. The wound-free control group (without a wound) and wounded group (BHG-untreated) corneoscleral rings were placed in 2 mL of low serum-free medium 199 containing 1% antibiotic–antimycotic solution and cultured at 37 °C in a humidified 5% CO₂ incubator for 0, 24, 48, and 72 h (Fig. 1D). Throughout the experiment, the culture plates were kept moistened by constant pouring of complete medium at the limbal border and surface of the epithelium every 4 h until the end of the experiment. The study was repeated three times for each cornea (total number of corneas, n = 24).

Tissue processing for light microscopy (histology) and electron microscopy

The organ-cultured corneoscleral rings were cut into two halves: one half of the corneoscleral ring was processed for light microscopy, and the other half was processed for electron microscopy. For light microscopy, the tissues were fixed for 48 h in 10% formalin (FA) in PBS. The tissue was washed in 0.1M PBS, dehydrated in a graded series of ethanol-xylene, and embedded in paraffin wax. Paraffin Sects. (5 µm thickness) were cut with a Remi microtome and collected on polysine-coated microscope slides (Lot # 100710-9, Thermo Scientific, Braunschweig, Germany). The sections were deparaffinized in xylene and rehydrated using a series of graded ethanol solutions. The sections were stained with hematoxylin and eosin and assessed under an Olympus BX51 bright field microscope using CellSens Entry Version 4.2 (Imaging Software, Olympus, Tokyo, Japan; CellSens V4.2 64bit Installer | Olympus LS (olympus-lifescience.com)).

The second half of the corneoscleral ring was fixed in 2.5% glutaraldehyde in 0.1 M PBS for electron microscopy. The tissue was washed with 0.1 M PBS and post-fixed in 1% osmium tetroxide for one hour. They were then washed with distilled water and dehydrated in a graded series of ethanol solutions. Tissues were infiltrated with spur resin and embedded in spur resin at 70°C for 8 h. Ultrathin sections were cut using an RMC ultra-cut microtome XL (Reichert-Jung Ultra-cut Microtome, Tucson, AZ, USA) and stained with 2% uranyl acetate and lead citrate. Sections were observed under a JOEL 1400 transmission electron microscope (JEOL, Akishima, Japan). Digital images were captured using a bottom-mounted Quemesa camera and analyzed using the iTEM software (Soft Imaging System, Munster, Germany; iTEM Main Brochure 12_br_us_mk_EZ_fv.indd (ku.dk)).

Confocal fluorescence staining of corneal epithelial cell regeneration

Tran et al.²⁶ previously used the Nile red stain in differentiated adipocytes to confirm that lipid layers and particles are present in the plasma membrane and cytoplasm. This is one of the best methods for identifying progenitor fatty cells' proliferation and differentiation. Therefore, we used Nile red and DAPI staining to identify whether the cytoplasm contained lipid particles from regenerated epithelial cells in the wounded corneas. Briefly, tissue sections were deparaffinized, rehydrated, and rinsed with PBS at room temperature for five minutes each. After 30 min of incubation in Nile red solution (5 µg/mL) at room temperature, the tissue sections were washed with PBS for 5 min. 4',6-Diamidino-2'-phenylindole dihydrochloride (DAPI) was then added to PBS (2 µg/mL) and incubated for 10 min at room temperature. The slides were washed with PBS and mounted with Aquatex® (HC440258, Merck, Germany) before being examined under a Zeiss confocal fluorescence microscope with blue (ex/em: 358/461 nm) and red (ex/em: 586/617 nm) filters (LSM 990, Zeiss, Germany). Images were acquired using a Rolera Qimaging camera. The images were analyzed using Zeiss Zen lite 3.11 imaging Software (ZEN 3.11—Software Manual.pdf).

Immunohistochemical staining

Paraffin Sections (5 µm thickness) on polysine-coated glass slides were deparaffinized in xylene, rehydrated in alcohol and water gradients, and blocked with 3% hydrogen peroxide (H₂O₂) in 50% methanol for 15 min. Slides were incubated in trisodium citrate buffer (pH 6) for ten minutes at 100°C for heat-induced epitope retrieval. Sections were washed with PBS and blocked with goat serum (3%, v/v) for one hour at room temperature. The sections were incubated overnight at 4°C with primary antibodies against fibronectin (1:100), α-SMA (1:200), and Ki67 (1:200). The sections were then washed with PBS-Tween 20 (PBST) for 5 × 3 min, followed by incubation with HRP-conjugated secondary goat anti-rabbit antibody (1:50) for one hour at room temperature. After PBST washing, the tissues were incubated with freshly prepared 3,3'-diaminobenzidine tetrahydrochloride (DAB, Sigma-Aldrich, Germany) with substrates (1:30) for approximately 8 min and checked microscopically for correct staining levels. After that, the slides were rinsed with tap water to stop the DAB reaction, counterstained

with hematoxylin for four minutes, washed, dehydrated with alcohol and xylene gradients, and mounted with Aquatex® (HC440258, Merck, Germany). Images were captured using CellSens Entry Version 4.2 (Imaging Software, Olympus, Tokyo, Japan) on an Olympus BX51 bright field microscope.

Statistical analysis

The obtained data were used to calculate the Mean \pm Standard Error (SE), and statistical analysis was performed using GraphPad Prism 8.2 tools (GraphPad Software, San Diego, CA, USA; Prism 8.2.0 Release Notes (graphpad.com)). The datasets were analyzed using the Mann–Whitney unpaired t test. The P values obtained through the Mann–Whitney unpaired T test for multiple comparisons that were less than 0.05, 0.01, 0.001 are represented by *, **, *** compared to those of the group that was not subjected to wounding.

Results

Histological evaluation of BHG-treated corneas

H&E staining is the primary assay used to analyze wound healing and epithelial regeneration in ex vivo organ-cultured corneas. Morphological abnormalities were confirmed by physical examination of histological specimens using H&E stain. In Fig. 2A, the camel peripheral-central corneal epithelium and anterior stroma are shown in the control corneas. In the wound-created cornea shown in Fig. 2B, the epithelium was peeled off from the corneal tissue before the experiments were conducted. After 24 h, corneal tissue sections from the wounded and wounded with BHG-treated corneas are shown in Fig. 2C,D. BHG treatment caused corneal regeneration on the first day, with epithelial cells migrating from the wound edge to fill the gap (Fig. 2D). Figure 2E shows the newly generated epithelium in the wounded corneas at 48 h after wounding. As shown in Fig. 2F, after 48 h of BHG treatment, the wound closed as the epithelial cells were pushed further over the anterior stroma. After 72 h, Fig. 2G,H show wounded corneas and wounded corneas treated with BHG. A thin epithelial layer completely covered the wounded stroma. Still, in the BHG-treated cornea (Fig. 1H), the inner stromal cells moved towards the anterior stroma and were covered with a thick epithelial layer. As shown in Fig. 2I and J, graphs of wound size (mm) and wound healing rate (mm²/h) were significantly improved in BHG-treated corneas, when compared to those in wounded (untreated) corneas at 24, 48, and 72 h.

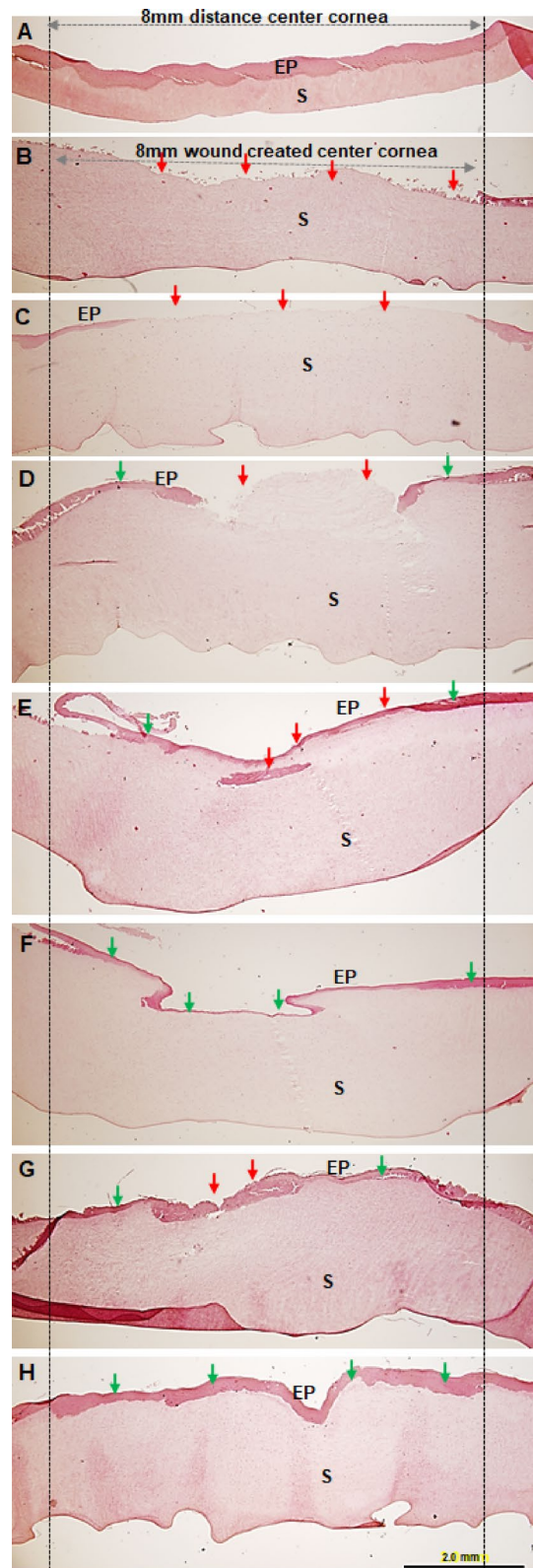
Evaluation of regenerated epithelial cell lineage

In this study, Nile red staining was used to evaluate newly regenerated and differentiated cells in wounded corneas and corneas treated with BHG. In contrast, DAPI staining was used to determine the nuclear morphology and induction of apoptosis. In Fig. 3A and B, representative confocal fluorescence microscopic images of control and wounded corneas stained with Nile red (red color) and DAPI (blue color). Compared to that in merged image of control corneas in Fig. 3A, which shows stroma with epithelium and nuclei, the merged image of wounded corneas in Fig. 3B shows stroma without epithelium and cellular nuclei. In Fig. 3C,D, corneal tissue sections were examined 24 h after being wounded with BHG treatment. Figure 3D shows high regeneration and migration of immature cells on the superficial stroma in BHG-treated cornea, but very little in wounded (untreated) corneas, as shown in Fig. 3C. In both wounded and BHG-treated corneas, re-epithelialization was observed after 48 h (Fig. 3E and F). BHG-treated corneas showed increased epithelialization (Fig. 3F) compared to that in wounded corneas (Fig. 3E). In both wounded and BHG-treated corneas, extensive corneal re-epithelialization was observed at 72 h (Fig. 3G and H). Trans-differentiation of inner stromal cells and migration of epithelial cells were increased in BHG-treated corneas, as shown in Fig. 3H. Overall, the arrows in Fig. 3H demonstrate that the amount of trans-differentiation and migration of the epithelial cell lineage is high in the superficial stroma of the corneas treated with BHG, but not in wounded (untreated) corneas (Fig. 3G).

Ultrastructure of control, wounded, and BHG-treated wounded corneas

The control camel cornea contained the glycocalyx on the surface of the squamous cells, followed by wing cells and basal epithelial cells, which contained tonofilaments and nuclei (Fig. 4A). The basal epithelial cells were attached to the basement membrane by the hemidesmosomes (Fig. 4B). Collagen fibrils in the anterior stroma were organized and had regular interfibrillar spacing. The wounded cornea showed the development of basal epithelial cells, but not squamous cells or wing cells, 72 h after the wound was created (Fig. 4C). These cells contained the nucleus and tonofilaments and were attached to the basement membrane by hemidesmosomes (Fig. 4D,E). The basement membrane was followed by the anterior stroma, which contained loosely arranged collagen fibrils (Fig. 4F). The structure of the CFs was not normal, and there was a large interfibrillar spacing between them (Fig. 4F).

After 72 h, the wounded with BHG-treated cornea, epithelium developed throughout the corneal wound. At the early stages of BHG treatment, the epithelial cells were not very well developed. Still, they gradually started to develop, and after 72 h of BHG treatment, the epithelium and basement were fully developed (Fig. 5A). The microvilli of the epithelium were well-developed on the surface of the squamous cells, and the glycocalyx was present on the surface of the microvilli (Fig. 5A–C). It appears that the glycocalyx oozed from the microvilli. The layers of squamous cells, wing, and basal epithelial cells were organized and contained normal organelles (Fig. 5C). Squamous cells and wing cells were connected to each other by desmosomes and tight junctions (Fig. 5A,B). The basal epithelial cells contained tonofilaments that were connected to each other by desmosomes (Fig. 6A). These basal epithelial cells were attached to a well-developed basement membrane by hemidesmosomes (Fig. 6A,B). The basement membrane was composed of two layers: lamina lucida and lamina densa (Fig. 6B). The basement membrane was not fully developed in some areas of the central wound. The basement membrane was connected to collagen fibrils, which ran randomly in the anterior stroma (Fig. 6B). Collagen fibrils in the anterior stroma were uniformly organized (Fig. 6C).



Immuno-localization of fibronectin, α -smooth muscle actin (α -SMA), and Ki-67

As shown in Fig. 7A, fibronectin immuno-labeling was moderately intense in the control corneal epithelium but not in the wounded corneal superficial stroma (Fig. 7B). Figure 7D shows that the BHG treatment accelerates the stimulation of fibronectin in the corneal superficial stroma upon 24 h of incubation, as compared to untreated wounded corneas (Fig. 7C). In wounded corneas treated with BHG at 48 and 72 h (Fig. 7F and H), the intensity of fibronectin antibody labeling in the epithelium was greater than that in untreated wounded corneas (Fig. 7E and G). Similarly, Figs. 8A and B show that the α -SMA antibody does not accumulate in the control and wounded corneal epithelium and stroma. In Fig. 8C, wounded corneas without BHG treatment

◀ **Fig. 2.** Light micrograph representing hematoxylin and eosin (H&E) stained tissue sections in control, wounded, and wounded with BHG-treated camel corneas at 0, 24, 48, and 72 h. (A) Representative image of peripheral-center cornea in control with clear epithelium and stroma; (B) Representative image of wound-created center corneas with peeled epithelium, superficial stroma; (C) Representative image of wounded center cornea at 24 h; (D) Representative image of wounded with BHG-treated center cornea at 24 h, epithelium on each edge of wounds started regenerating and migrated towards the corneal superficial stroma; (E) An image representative of the wounded center cornea at 48 h, where a thin epithelia covers the superficial stroma with scarring; (F) Representative image of a wounded with BHG-treated center cornea at 48 h, where a thin epithelium covered the superficial stroma without scarring; (G) Representative image of the wounded center cornea at 72 h, where the multilayer epithelial covered the superficial stroma with scarring; (H) Representative image of the wounded with BHG-treated center cornea at 72 h, where multilayer epithelium covered completely the superficial stroma without scarring. The images were all captured at $2\times$ magnification (scale bar = 2 mm). (I and J) The graph shows the wound size (mm) and wound healing rate (mm^2/h) in center corneas analyzed by image J software. Three replicates were conducted for each experiment ($n = 3$). The data are presented as the mean \pm standard error (S.E.). The P values obtained through the Mann-Whitney unpaired T test for multiple comparisons that were less than 0.05, 0.01, 0.001 are represented by *, **, *** compared to those of the group that was not subjected to wounding. EP-epithelium, S-stroma, Green arrow-showing newly regenerated cells and red arrows shows unregenerate and epithelium with scarring in the wounded corneas.

stimulate antibody labeling in the superficial stroma upon 24 h of incubation, as opposed to wounds with BHG treatment (Fig. 8D). Moreover, the staining intensity of α -SMA antibody labeling was greater in untreated wounds than in wounded corneas treated with BHG at 48 and 72 h (Fig. 8E–H). α -SMA antibody labeling was highly intense in the scarring area of untreated wounded corneal epithelium at 48 and 72 h incubation. In addition, the proliferation factor ki-67 antibody immunolabelling occurred moderately in the control corneal basal epithelium (Fig. 9A), but not in the wounded corneal superficial stroma (Fig. 9B). As shown in Fig. 9C, wounded corneas without BHG treatment didn't show any ki-67 antibody-labeled cells after 24 h incubation, but wounds treated with BHG promoted ki-67-positive cells in the superficial stroma (Fig. 8D). Then, corneas treated with BHG at 48 and 72 h show increased staining intensity of the ki-67 antibody-labeled basal cells in the regenerated epithelium (Fig. 9F and H), when compared to untreated wounded corneas (Fig. 9E and G). These results may represent the proliferation and trans differentiation of fibroblasts into epithelial-like cell lineages on the surface of the wounded corneas.

Discussion

In this study, BSA-formulated hydrogels (BHG) were prepared in several phases for optimization. Previously, the rapid cross-linking gelation method relied on a higher volume of glutaraldehyde, which caused toxicity. To prevent toxicity and adverse effects, we have revised the modified gelation method. BHG was synthesized using a low volume of glutaraldehyde (2.5%) and BSA (5, 10%, and 20%; Fig. 1) formulations. This experiment assessed the effect of 10% BHG (BSA-formulated with retinoic acid and riboflavin hydrogel) on the wounded epithelium of camel corneal rims at 0, 24, 48, and 72 h. The histological results showed that BHG treatment at 48 and 72 h increased the development of epithelial cells and stromal CFs. Similarly, our ultrastructural studies revealed that the epithelium was partially developed in the cornea 72 h after wounding, whereas it was fully developed in the wounded cornea 72 h after BHG treatment. The collagen fibrils were well-organized and uniformly distributed. Furthermore, Nile red and DAPI staining confirmed the proliferation and migration of regenerated epithelial cells propagating through the corneal epithelium in BHG-treated corneas. Treatment with BHG in wounded corneas resulted in a lower level of α -SMA and a high level of fibronectin and ki-67 staining appeared after 48 and 72 h, signifying the repair of the epithelium.

Corneal injury can damage the epithelium and basement membrane. Injury to the epithelium leads to the release of numerous excretory molecules, such as interleukins/cytokines, growth factors, and inflammatory proteins, which stimulate fibroblasts²⁷. These stimulated fibroblasts migrate to damaged tissues and transform into myofibroblasts, which release extracellular matrix proteins and low levels of α -SMA to restore tissue integrity²⁸. Injury involving damage to the basement membrane (BM) leads to the penetration of pro-fibrotic cytokines, such as transforming growth factor (TGF), and the production of high levels of mature α -SMA-positive myofibroblasts that lead to scarring and stromal fibrosis²⁹. BM damage leads to the development of myofibroblasts that persist in the corneal stroma³⁰. Keratocytes transition into fibroblasts in the wound area, and these fibroblasts are induced to differentiate into myofibroblasts by the production of TGF- β and PDGF. Degenerative epithelial BMs regenerate after corneal injury due to the development of myofibroblasts from keratocyte-derived precursor cells²⁹. Degeneration of the BM triggers and releases epithelial-derived transforming growth factor beta (TGF- β), platelet-derived growth factor (PDGF), and other modulators to penetrate the stroma²⁹. The release of TGF- β and PDGF initiates vimentin, alpha smooth muscle actin (α -SMA), desmin, and myofibroblasts³¹. In the present study, the low level of α -SMA and high level of fibronectin antibody staining in BHG-treated corneas revealed the repair of the epithelium and stroma at 48 and 72 h.

Cheng et al.³² studied the antibacterial properties of a BSA-formulated hydrogel against multidrug-resistant *S. aureus* bacteria during wound healing. The authors suggested that BSA-formulated hydrogels can also retain and transport large volumes of water molecules owing to their hydrophilic nature, which increases corneal repair and its biomechanical properties. Later, Kong et al. 2023 reported that albumin-based hydrogel scaffolds can promote re-epithelialization of the cornea³³. Similarly, our present results showed that BHG could repair damaged corneas by promoting epithelial and stromal cell regeneration without altering the microarchitecture,

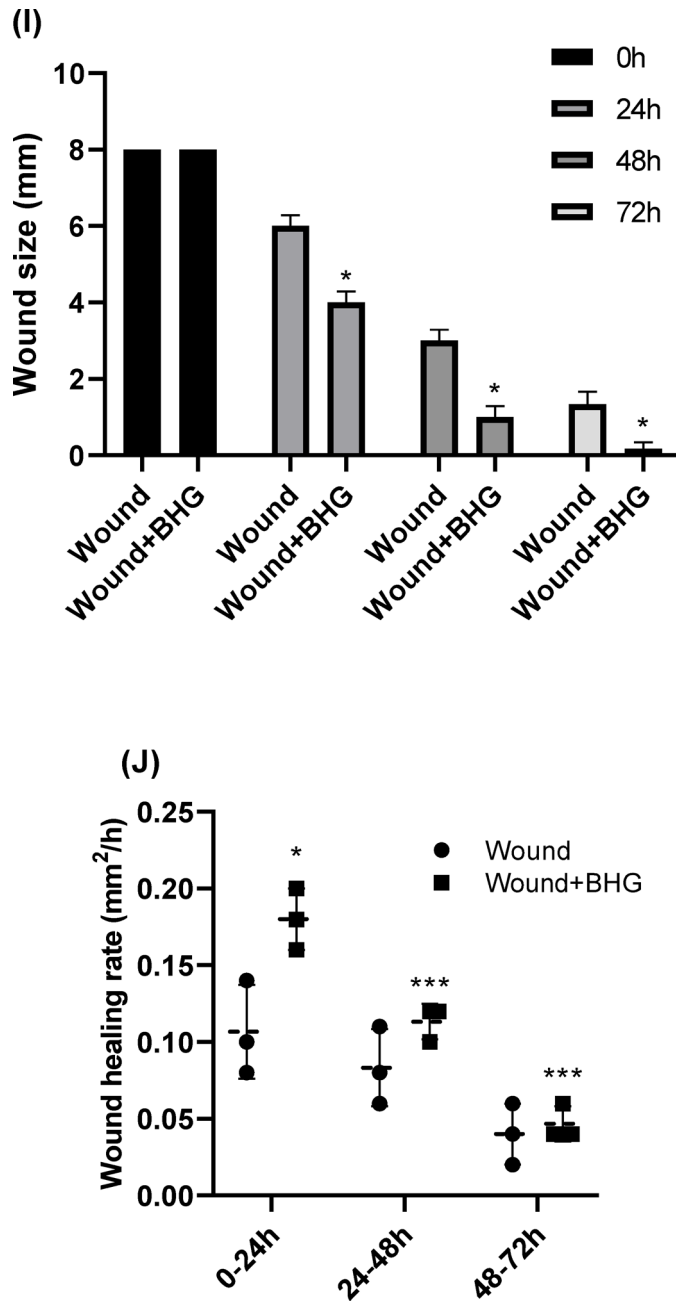


Fig. 2. (continued)

as reported by Kong et al.³³. We believe that BHG also has antimicrobial, anti-contamination, and biodegradable properties and controls the release of small molecules, as previously reported³².

Additionally, we also investigated Ki-67 immunohistochemical staining in wounded and wound-healed corneas, since Ki-67 is a well-known proliferation marker for corneal re-epithelialization. Results showed that wounds with BHG-treated corneas showed a significant amount of ki-67 positivity labeled basal cells at 48 and 72 h, indicating that it promotes re-epithelialization. A previous study by Li et al. 2023 reported that rhFGF-21 treatment of diabetic mice with wounded corneas upregulated Ki-67 levels, which induced basal cell proliferation and re-epithelialization³⁴. It was also found that high levels of Ki-67 expression in corneal epithelial cells resulted in higher migration and proliferation activity during corneal wound healing³⁵. Similarly, RF in the hydrogel formulation upregulates the transglutaminase-2 (TG2) enzyme, which enhances wound healing, adhesion, proliferation, and migration of epithelial cells, as reported previously⁸⁻¹⁰. The inclusion of RA promotes the upregulation of Wnt- β -catenin signaling, which is involved in the regeneration of corneal stromal cells¹⁵. These results may support further in vivo studies with BHG-formulated biomaterials and preservation of corneal microarchitecture under pathological conditions.

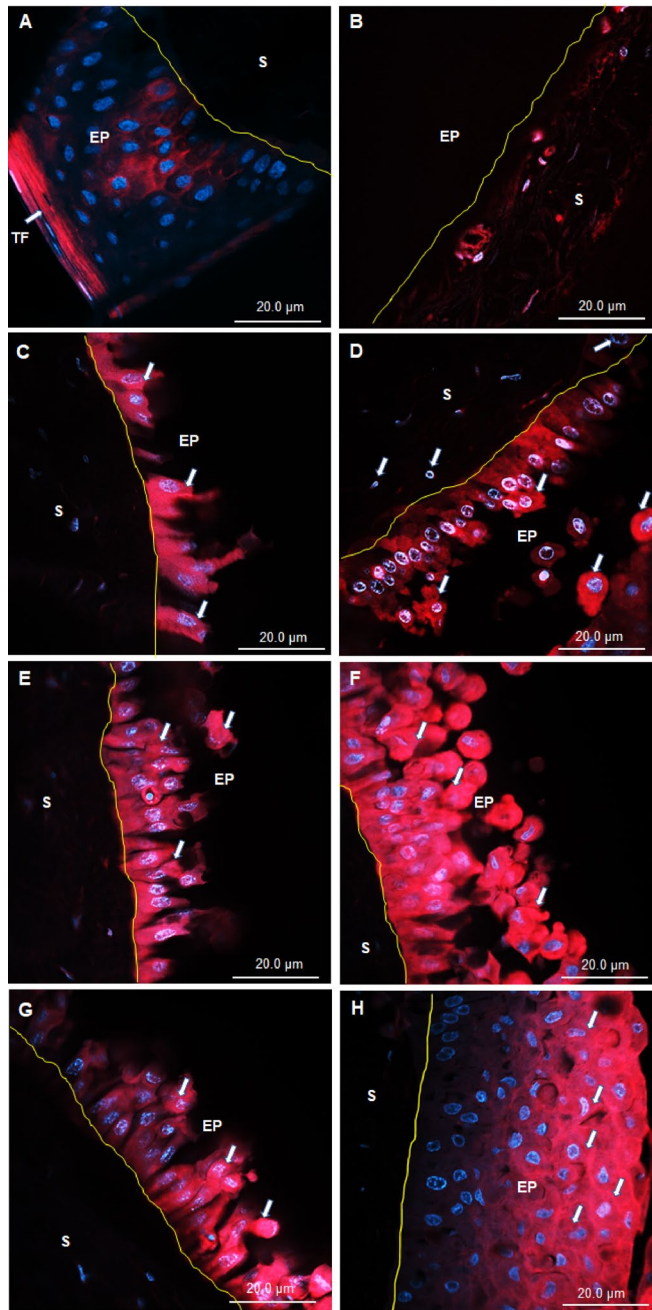


Fig. 3. The Nile red/DAPI stained at 24, 48, and 72 h, regenerated epithelium, and differentiated epithelial lineages in wounded and BHG-treated corneas were captured by confocal fluorescence microscopy. In ex vivo organ-cultured sections from control, wounded, and BHG-treated camel corneas, Nile red stain (red color) was labeled in the cell membrane and cytoplasm, and DAPI stain (blue color) was labeled in the nuclei. **(A)** Control cornea with epithelium, tear film and superficial stroma; **(B)** 0-h wounded cornea without epithelium; **(C)** 24 h wounded cornea; **(D)** 24 h wounded with BHG-treated corneas merged image shown newly regenerated cells with and without nuclei; **(E)** 48 h wounded corneas merged image shown less newly regenerated cells with nuclei; **(F)** 48 h wounded with BHG-treated corneas merged image shown newly regenerated cells with and without nuclei; **(G)** 72 h wounded corneas merged image shown less newly regenerated cells and cell nuclei; **(H)** 72 h wounded with BHG-treated corneas merged image shown newly regenerated cells differentiated into epithelial cell lineages. The images were all captured of the center corneas at 40× magnification (scale bar = 20 μm). The merged images in center corneas were used Zeiss Zen lite 3.11 software. Three replicates were conducted for each experiment (n = 3). White arrow -Nile red staining showing newly regenerated cells (red color) with nuclei (blue color). E-epithelium, S-stroma, TF-tear film.

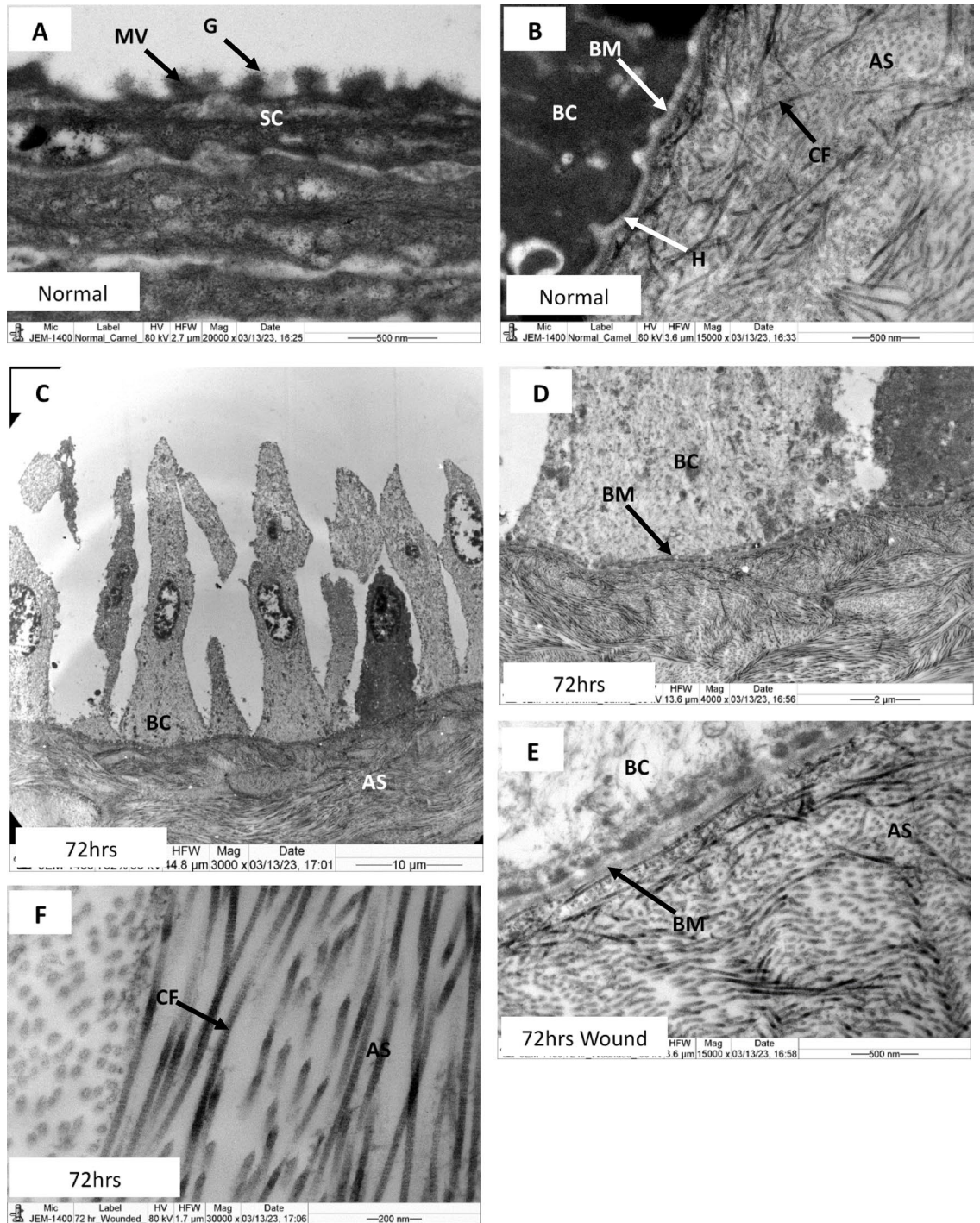


Fig. 4. Electron micrograph of a control at 0 h and 72 h wounded organ culture camel cornea; **(A)** Part of the surface of the epithelium in control cornea showing the glycocalyx on the surface of the microvilli; **(B)** Part of the epithelium of control cornea showing basal epithelial cells, basement membrane, hemidesmosomes and collagen fibrils; **(C)** Part of the epithelium of 72 h wounded cornea showing developing basal epithelial cells. Note that there are no squamous cells, and wing cells; **(D and E)** Part of the epithelium 72 h wounded cornea showing basal epithelial cells, basement membrane, hemidesmosomes and collagen fibrils. **(F)** Part of the anterior stroma of 72 h wounded cornea showing irregularly distributed collagen fibrils. AS-anterior stroma, BC-basal epithelial cells, BM-basement membrane, D-desmosomes, CF-collagen fibrils, G-glycocalyx, MV-microvilli, N-nucleus, SC-squamous cells, WC-wing cells.

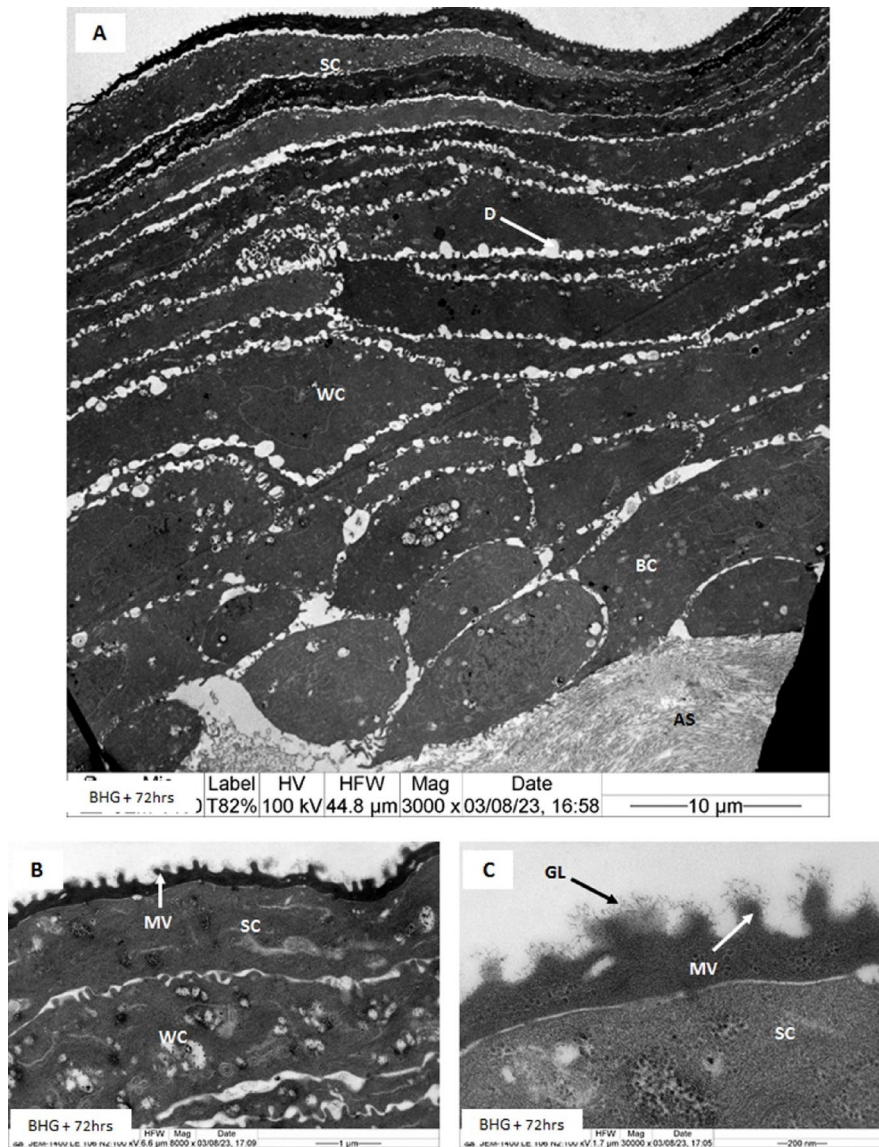


Fig. 5. Electron micrograph of wounded with BHG-treated at 72 h organ culture camel cornea; (A) Part of the corneal epithelium showing layers of well-developed squamous cells, wing cells, basal cells and microvilli on the surface of squamous cells; (B and C) Part of the epithelium showing deposition of glycoalyx droplets on the surface of microvilli, similar to the control cornea. AS-anterior stroma, D-desmosomes, BC-basal epithelial cells, G-glycoalyx, MV-microvilli, SC-squamous cells, WC-wing cells.

The ex vivo organ culture wound healing model has some limitations. (1) It is difficult to handle an airway culture system because epithelial cells have an inadequate cell passage. (2) In an ex vivo model, the whole cornea acts as a reservoir to supply niche factors via the limbus and stromal crowded cell migration toward the wounded surfaces. (3) It is difficult to maintain sterility, prevent swelling, and prevent superficial cell damage in long-term culture as well as in the absence of antibiotics. (4) Camel corneas are more affordable than other ex vivo corneal organ culture models because of their wide and multilayer epithelium thickness. (5) Therefore, we believe that camel corneas are the most suitable model for testing the efficacy of drug delivery systems in boosting epithelial recovery during wound healing and re-epithelialization.

In summary, our study revealed that BHG treatment regulates corneal epithelial cell regeneration and differentiation in the anterior stroma by upregulating fibronectin and Ki-67 proteins and downregulating α -SMA protein. It promotes the proliferation of epithelial cells and inhibits corneal fibrosis through the inclusion of RF and RA in the BHG. According to these results, stromal keratocyte degeneration was prevented in BHG-treated corneas but not in untreated wounded corneas. Overall, these findings demonstrate that BHG plays a significant role in corneal homeostasis, strengthening epithelial cell regeneration and proliferation. An ex vivo corneal wound healing study may serve as a platform for developing regenerative medicine-based therapeutic strategies for corneal diseases. Still, it may also aid in adding more detail to an in vivo study.

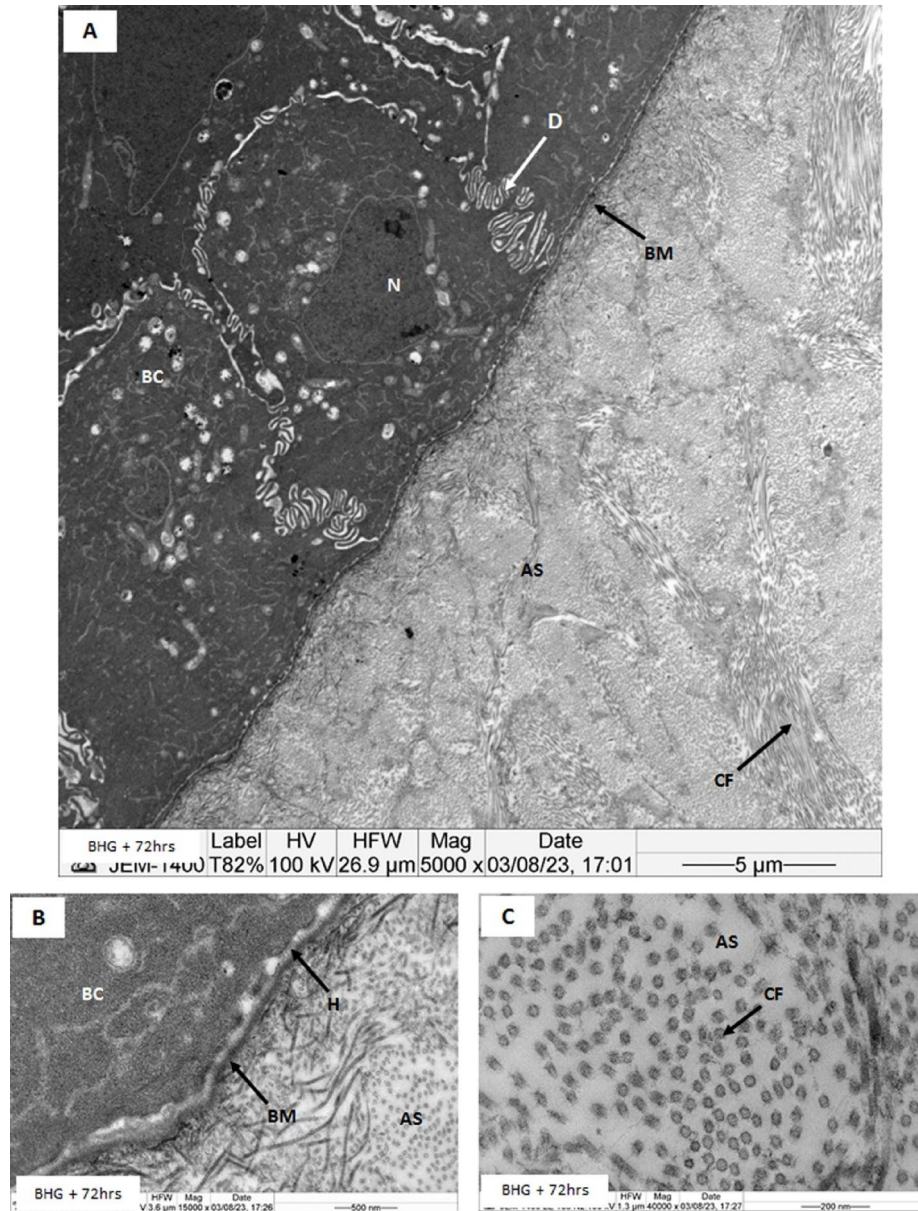


Fig. 6. Electron micrograph of wounded with BHG-treated 72 h organ culture camel cornea; **(A)** Part of the cornea showing basal epithelial cells, basement membrane, hemidesmosomes and collagen fibrils in the anterior stroma; **(B)** Part of the basement membrane showing well-developed hemidesmosomes; **(C)** Part of the anterior stroma showing irregularly distributed collagen fibrils. AS-anterior stroma, BC-basal epithelial cells, CF-collagen fibrils, D- desmosomes, H-hemidesmosomes, N-nucleus, SC-squamous cells, WC-wing cells.

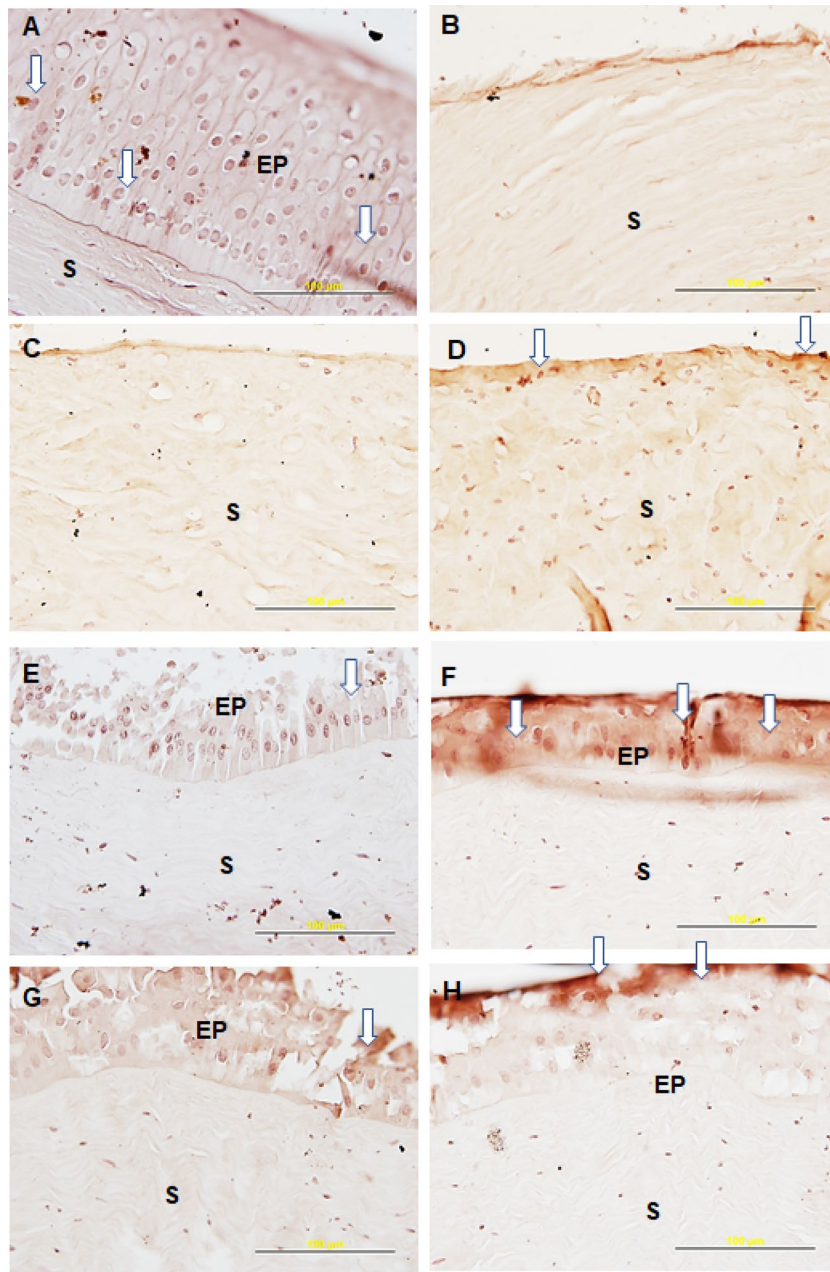


Fig. 7. Immunohistochemical staining of fibronectin in control, wounded, and BHG-treated organ culture camel corneas; **(A)** Control cornea with epithelium shown fibronectin antibody labeled in basal epithelial cells; **(B)** Wounded cornea without epithelium shown lacking fibronectin antibody labeling; **(C)** 24 h wounded cornea shown lacking fibronectin antibody labeling; **(D)** 24 h wounded with BHG-treated corneas shown fibronectin antibody labeled cells on superficial stroma; **(E)** 48 h wounded corneas shown weakly fibronectin antibody labeled positive cells in the regenerated epithelium; **(F)** 48 h wounded with BHG-treated corneas shown strong fibronectin antibody labeling in the basal cell layers; **(G)** 72 h wounded corneas shown moderate fibronectin antibody labeling on the top of epithelium; **(H)** 72 h wounded with BHG-treated corneas shown strong fibronectin antibody labeling on the top of epithelium. The images were all captured from center corneas at 60× magnification (scale bar = 100 μm). Three replicates were conducted for each experiment (n = 3). EP-epithelium, S-stroma, and Arrows are showing newly regenerated cells with fibronectin antibody-stained positive cells.

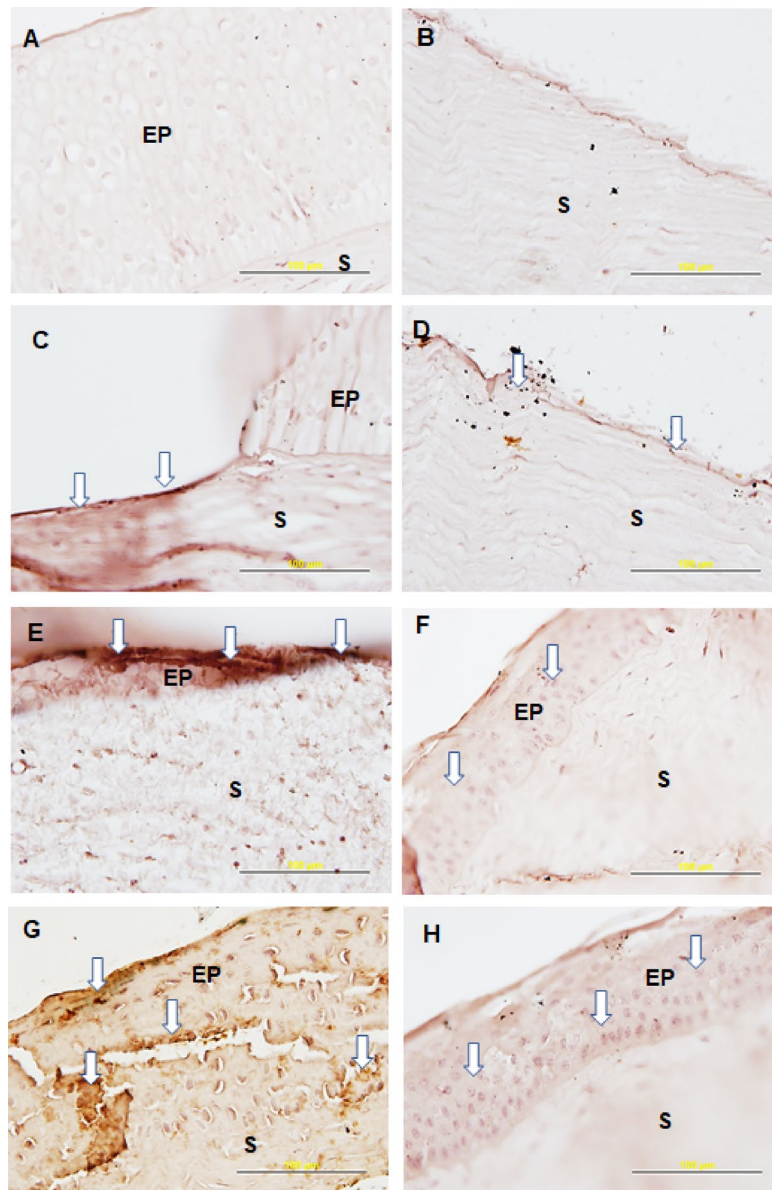


Fig. 8. Immunohistochemical staining of smooth muscle actin (α -SMA) in control, wounded, and BHG-treated organ culture camel corneas; (A) Control cornea with epithelium shown lacking α -SMA antibody labeling in the epithelium and stroma; (B) Wounded cornea without epithelium shown lacking α -SMA antibody labeling in the superficial stroma; (C) 24 h wounded cornea shown strong α -SMA antibody labeling on the top of superficial stroma; (D) 24 h wounded with BHG-treated cornea shown mild α -SMA antibody labeling on the top of superficial stroma; (E) 48 h wounded cornea shown very strong α -SMA antibody labeling in the epithelium; (F) 48 h wounded cornea shown lacking α -SMA antibody labeling in the epithelium; (G) 72 h wounded cornea shown strong α -SMA antibody labeling in the scarred areas of epithelium and superficial stroma; (H) 72-h wounded with BHG-treated cornea shown lacking α -SMA antibody labeling in the epithelium and superficial stroma. The images were all captured from the center cornea at 60 \times magnification (scale bar = 100 μ m). Three replicates were conducted for each experiment (n = 3). EP-epithelium, S-stroma, and Arrows show newly regenerated epithelium and superficial stroma with α -SMA antibody labeling.

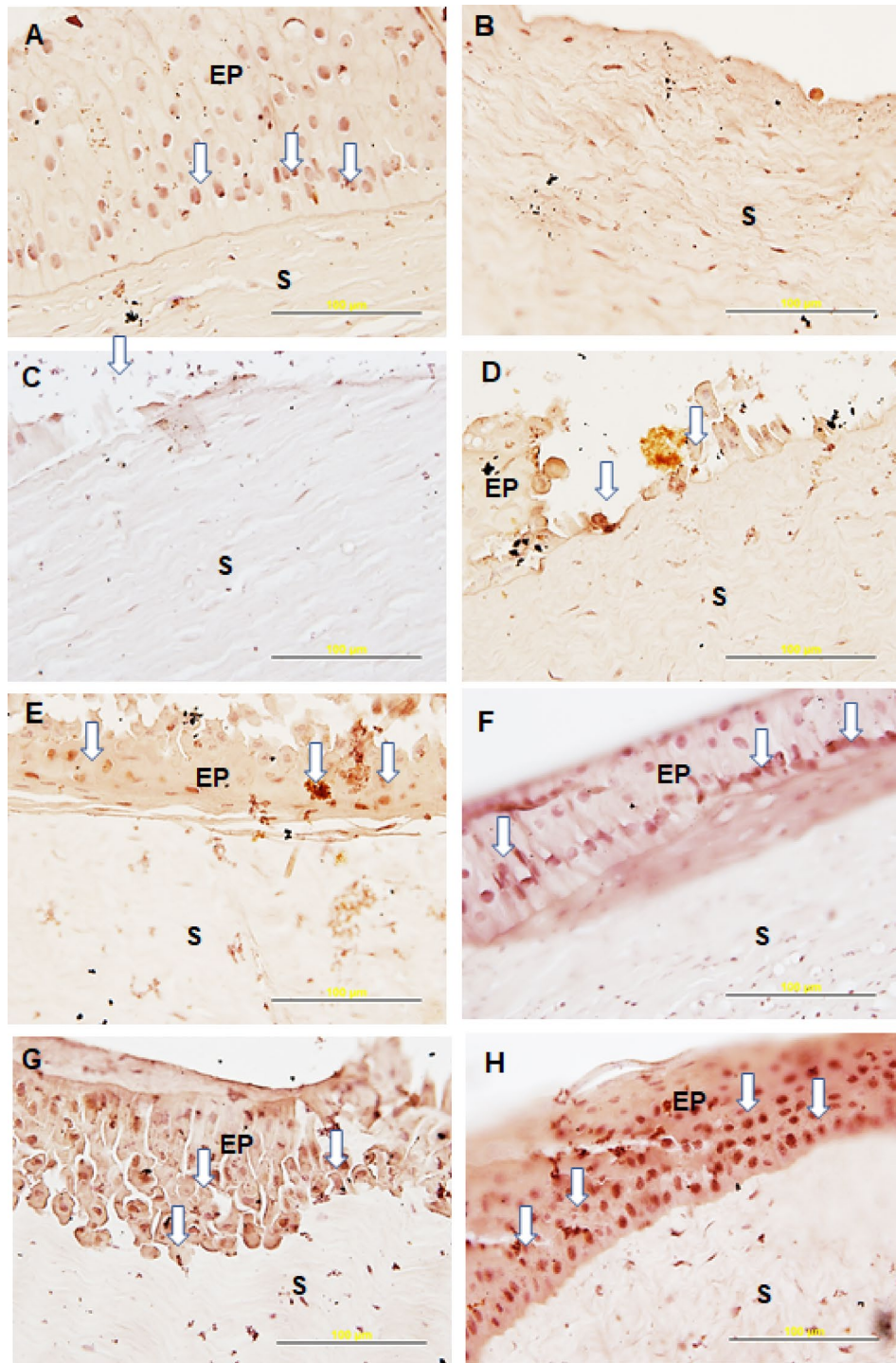


Fig. 9. Immunohistochemical staining of Ki-67 in control, wounded, and BHG-treated camel corneas; (A) Control cornea with epithelium shown Ki-67 antibody labeled in basal epithelial cells; (B) Wounded cornea without epithelium shown lacking Ki-67 antibody labeling; (C) 24 h wounded cornea shown very few Ki-67 antibody labeling in the edge of corneal wounds; (D) 24 h wounded with BHG-treated cornea shown few Ki-67 antibodies labeled basal cells in edge of corneal wounds and top of superficial stroma; (E) 48 h wounded cornea shown few Ki-67 antibody labeling in the regenerated basal cells; (F) 48 h wounded with BHG-treated cornea shown Ki-67 antibody labeling in regenerated epithelium basal cells; (G) 72 h wounded cornea shown moderate Ki-67 antibody labeling in the regenerated epithelium; (H) 72 h wounded with BHG-treated cornea shown strong Ki-67 antibody labeling in the regenerated epithelium and basal cells. The images were all captured from the center cornea at 60× magnification (scale bar = 100 µm). Three replicates were conducted for each experiment (n = 3). EP-epithelium, S-stroma, and Arrows show newly regenerated epithelium and basal cells in Ki-67 antibody-labeled positive cells.

Data availability

The original contributions presented in this study are included in this manuscript. Further inquiries can be directed to the corresponding author.

Received: 12 May 2024; Accepted: 27 May 2025

Published online: 06 June 2025

References

1. Sklenarova, R., Akla, N., Latorre, M. J., Ulrichova, J. & Frankova, J. Collagen as a biomaterial for skin and corneal wound healing. *J. Funct. Biomater.* **13**(4), 249. <https://doi.org/10.3390/jfb13040249> (2022).
2. Kamil, S. & Mohan, R. R. Corneal stromal wound healing: Major regulators and therapeutic targets. *Ocul. Surf.* **19**, 290–306. <https://doi.org/10.1016/j.jtos.2020.10.006> (2021).
3. Cheng, X., Petsche, S. J. & Pinsky, P. M. A structural model for the in vivo human cornea including collagen-swelling interaction. *J. R. Soc. Interface* **12**(109), 20150241. <https://doi.org/10.1098/rsif.2015.0241> (2015).
4. Almubrad, T. & Akhtar, S. Ultrastructure features of camel cornea—collagen fibril and proteoglycans. *Vet. Ophthalmol.* **15**(1), 36–41. <https://doi.org/10.1111/j.1463-5224.2011.00918.x> (2011).
5. Torricelli, A. A., Singh, V., Santhiago, M. R. & Wilson, S. E. The corneal epithelial basement membrane: Structure, function, and disease. *Invest. Ophthalmol. Vis. Sci.* **54**(9), 6390–6400. <https://doi.org/10.1167/iovs.13-12547> (2013).
6. Kruegel, J. & Miosge, N. Basement membrane components are key players in specialized extracellular matrices. *Cell Mol. Life Sci.* **67**, 2879–2895. <https://doi.org/10.1007/s00018-010-0367-x> (2010).
7. Jia, H. Z. & Peng, X. J. Efficacy of iontophoresis-assisted epithelium-on corneal cross-linking for keratoconus. *Int. J. Ophthalmol.* **11**(4), 687–694. <https://doi.org/10.18240/ijo.2018.04.25> (2018).
8. Wu, J., Wang, J., Wang, L. & Huang, Y. Topical retinoic acid induces corneal strengthening by upregulating transglutaminase 2 in murine cornea. *Exp. Eye Res.* **214**, 108850. <https://doi.org/10.1016/j.exer.2021.108850> (2022).
9. Png, E. & Tong, L. Transglutaminase-2 in cell adhesion: All roads lead to paxillin?. *Cell Adh. Migr.* **7**(5), 412–417. <https://doi.org/10.4161/cam.26344> (2013).
10. Tong, L. et al. Molecular mechanism of transglutaminase-2 in corneal epithelial migration and adhesion. *Biochim Biophys Acta* **1833**(6), 1304–1315. <https://doi.org/10.1016/j.bbamcr.2013.02.030> (2013).
11. Yu, Q. et al. Canonical NF- κ B signaling maintains corneal epithelial integrity and prevents corneal aging via retinoic acid. *Elife* **10**, e67315. <https://doi.org/10.7554/eLife.67315> (2021).
12. Abidin, F. Z., Gouveia, R. M. & Connon, C. J. Application of retinoic acid improves form and function of tissue engineered corneal construct. *Organogenesis* **11**(3), 122–136. <https://doi.org/10.1080/15476278.2015.1093267> (2015).
13. Gouveia, R. M. & Connon, C. J. The effects of retinoic acid on human corneal stromal keratocytes cultured in vitro under serum-free conditions. *Invest. Ophthalmol. Vis. Sci.* **54**(12), 7483–7491. <https://doi.org/10.1167/iovs.13-13092> (2013).
14. Lynch, A. P. & Ahearne, M. Retinoic acid enhances the differentiation of adipose-derived stem cells to keratocytes in vitro. *Transl. Vis. Sci. Technol.* **6**(1), 6. <https://doi.org/10.1167/tvst.6.1.6> (2017).
15. Smith, J. N. et al. Lens-regulated retinoic acid signaling controls expansion of the developing eye. *Development* **145**(19), dev167171. <https://doi.org/10.1242/dev.167171> (2018).
16. Kumar, S., Dollé, P., Ghyselinck, N. B. & Duester, G. Endogenous retinoic acid signaling is required for maintenance and regeneration of cornea. *Exp. Eye Res.* **154**, 190–195. <https://doi.org/10.1016/j.exer.2016.11.009> (2017).
17. Godoy-Parejo, C., Deng, C., Zhang, Y., Liu, W. & Chen, G. Roles of vitamins in stem cells. *Cell Mol. Life Sci.* **77**(9), 1771–1791. <https://doi.org/10.1007/s00018-019-03352-6> (2020).
18. Almubrad, T. et al. Ultrastructural study of collagen fibrils, proteoglycans and lamellae of the cornea treated with iontophoresis—UVA cross-linking and hypotonic riboflavin solution. *Saudi J. Biol. Sci.* **28**(12), 7160–7174. <https://doi.org/10.1016/j.sjbs.2021.08.019> (2021).
19. Sinha, T. et al. Riboflavin deficiency leads to irreversible cellular changes in the RPE and disrupts retinal function through alterations in cellular metabolic homeostasis. *Redox Biol.* **54**, 102375. <https://doi.org/10.1016/j.redox.2022.102375> (2022).
20. Bhattacharjee, P., Fernández-Pérez, J. & Ahearne, M. Potential for combined delivery of riboflavin and all-trans retinoic acid, from silk fibroin for corneal bioengineering. *Mater. Sci. Eng. C Mater. Biol. Appl.* **105**, 110093. <https://doi.org/10.1016/j.msec.2019.110093> (2019).
21. Ong, J., Zhao, J., Justin, A. W. & Markaki, A. E. Albumin-based hydrogels for regenerative engineering and cell transplantation. *Biotechnol. Bioeng.* **116**(12), 3457–3468. <https://doi.org/10.1002/bit.27167> (2019).
22. Jiang, H. & Xu, Z. Hyaluronic acid-based nanoparticles to deliver drugs to the ocular posterior segment. *Drug Deliv.* **30**(1), 2204206. <https://doi.org/10.1080/10717544.2023.2204206> (2023).
23. Bronze-Uhle, E. S., Costa, B. C., Ximenes, V. F. & Lisboa-Filho, P. N. Synthetic nanoparticles of bovine serum albumin with entrapped salicylic acid. *Nanotechnol. Sci. Appl.* **10**, 11–21. <https://doi.org/10.2147/NSA.S117018> (2016).
24. Karimi, M. et al. Albumin nanostructures as advanced drug delivery systems. *Expert Opin. Drug Deliv.* **13**(11), 1609–1623. <https://doi.org/10.1080/17425247.2016.1193149> (2016).
25. Castro, N., Gillespie, S. R. & Bernstein, A. M. Ex Vivo Corneal Organ Culture Model for Wound Healing Studies. *J. Vis. Exp.* (144). <https://doi.org/10.3791/58562> (2015).
26. Tran, C. T. et al. Adipose tissue can be generated in vitro by using adipocytes from human fat tissue mesenchymal stem cells seeded and cultured on fibrin gel sheet. *Cell Tissue Bank* **14**(1), 97–106. <https://doi.org/10.1007/s10561-012-9304-6> (2013).
27. Karin, M. & Clevers, H. Reparative inflammation takes charge of tissue regeneration. *Nature* **529**(7586), 307–315. <https://doi.org/10.1038/nature17039> (2016).
28. Klingberg, F., Hinz, B. & White, E. S. The myofibroblast matrix: Implications for tissue repair and fibrosis. *J. Pathol.* **229**(2), 298–309. <https://doi.org/10.1002/path.4104> (2013).
29. Wilson, S. E. Corneal myofibroblasts and fibrosis. *Exp. Eye Res.* **201**, 108272. <https://doi.org/10.1016/j.exer.2020.108272> (2020).
30. Wilson, S. E., Medeiros, C. S. & Santhiago, M. R. Pathophysiology of corneal scarring in persistent epithelial defects after PRK and other corneal injuries. *J. Ref. Surg.* **34**, 59–64. <https://doi.org/10.3928/1081597X-20171128-01> (2018).
31. Wilson, S. E., Sampaio, L. P., Shiju, T. M., Hilgert, G. S. L. & de Oliveira, R. C. Corneal opacity: Cell biological determinants of the transition from transparency to transient haze to scarring fibrosis, and resolution. *After Injury. Invest. Ophthalmol. Vis. Sci.* **63**(1), 22. <https://doi.org/10.1167/iovs.63.1.22> (2022).
32. Cheng, L. et al. Injectable polypeptide-protein hydrogels for promoting infected wound healing. *Adv. Func. Mater.* **30**(25), 2001196. <https://doi.org/10.1002/adfm.202001196> (2020).
33. Kong, F., Mehwish, N. & Lee, B. H. Emerging albumin hydrogels as personalized biomaterials. *Acta Biomater.* **157**, 67–90. <https://doi.org/10.1016/j.actbio.2022.11.058> (2023).
34. Li, L. et al. rhFGF-21 accelerates corneal epithelial wound healing through the attenuation of oxidative stress and inflammatory mediators in diabetic mice. *J. Biol. Chem.* **299**(9), 105127. <https://doi.org/10.1016/j.jbc.2023.105127> (2023).
35. Nagata, M. et al. JBP485 promotes corneal epithelial wound healing. *Sci. Rep.* **5**, 14776. <https://doi.org/10.1038/srep14776> (2015).

Acknowledgements

The authors extend their appreciation to the Deanship of Scientific Research, King Saud University, for funding through the Vice Deanship of Scientific Research Chairs, Research Chair of Cornea. We also express our gratitude for the support provided by the Scientific Research Unit, Inaya Medical Colleges, Saudi Arabia.

Author contributions

Conceptualization, R.S.; methodology, M.A.A., R.S., and A.A.K.; software, R.S. and S.A.; validation, M.A.A., R.S., A.A.K. and S.A.; formal analysis, M.A.A., R.S., and S.A.; investigation, R.S.; resources, S.A., S.A.A., A.M. and T.A.; data curation and re-analysis, M.A.A., R.S. and S.A.; writing-original draft preparation, R.S. and S.A.; writing-review and editing, S.A., S.A.A., A.M., and T.A.; visualization, R.S. and S.A.; supervision, R.S.; project administration, S.A.A., and S.A.; funding acquisition, S.A., S.A.A., A.M. and T.A. All authors have read and agreed to the published version of the manuscript.

Declarations

Competing interests

The authors declare no competing interests.

Additional information

Correspondence and requests for materials should be addressed to R.S. or S.A.

Reprints and permissions information is available at www.nature.com/reprints.

Publisher's note Springer Nature remains neutral with regard to jurisdictional claims in published maps and institutional affiliations.

Open Access This article is licensed under a Creative Commons Attribution-NonCommercial-NoDerivatives 4.0 International License, which permits any non-commercial use, sharing, distribution and reproduction in any medium or format, as long as you give appropriate credit to the original author(s) and the source, provide a link to the Creative Commons licence, and indicate if you modified the licensed material. You do not have permission under this licence to share adapted material derived from this article or parts of it. The images or other third party material in this article are included in the article's Creative Commons licence, unless indicated otherwise in a credit line to the material. If material is not included in the article's Creative Commons licence and your intended use is not permitted by statutory regulation or exceeds the permitted use, you will need to obtain permission directly from the copyright holder. To view a copy of this licence, visit <http://creativecommons.org/licenses/by-nc-nd/4.0/>.

© The Author(s) 2025